(16) Yamada, B.; Itahashi, M.; Otsu, T. *J. Polym. Sci.* **1978**, *16*, 1719.
(17) Patino-Leal, H.; Reilly, P. M.; O'Driscoll, K. F. *J. Polym. Sci., Part C* **1980**, *18*, 219.
(18) Reilly, P. M.; Patino-Leal, H. *Technometrics* **1981**, *23*, 221.
(19) Garcia-Rubio, L. H., Ph.D. Dissertation; McMaster University, 1981.
(20) Wentworth, W. E. *J. Chem. Educ.* **1965**, *42*, 96.
(21) The program was written in Fortran and is available on request from the authors.
(22) Sutton, T. L.; MacGregor, J. F. *Can. J. Chem. Eng.* **1977**, *55*, 602.
(23) Draper, N. R.; Smith, H. *Applied Regression Analysis*, 2nd ed.; Wiley: New York, 1981.

Computer Simulations of Radiation-Cured Networks

L. Y. Shy and B. E. Eichinger*

Department of Chemistry, BG-10, University of Washington, Seattle, Washington 98195.
Received June 17, 1986

ABSTRACT: Simultaneous cross-linking and chain scission reactions that are induced by ionizing radiation have been simulated with a computer. These studies were performed for both bulk- and solution-cured poly(dimethylsiloxane) (PDMS) systems. Variations of network structures and mechanical properties that depend on the degree of cross-linking are presented. It is shown that radiation-cured networks are barely connected and contain large amounts of defect structures. More than 90% of the defects are found to be dangling ends, and isolated ends are dominant in this population. The weight fraction of loops is quite small, but they deplete a large fraction of the cross-links. These results are in good agreement with experiment and with other calculations. Potential correlations between network structures and the Mooney–Rivlin coefficients $2C_1$ and $2C_2$ are also discussed.

1. Introduction

Networks that are cured through radiation-induced random cross-linking are of considerable commercial and laboratory interest. Numerous studies[1–8] have resulted in the characterization of the radicals that are formed, the yield of evolved gas, changes in viscosity, and the cross-linking densities of the networks. There is, however, much more to be understood. For instance, the extent and mechanism of backbone scission and rearrangement remain obscure. Moreover, we still do not know if network structures that have suffered radiation damage have altered dynamic mechanical properties.

Owing to the absence of analytical techniques for direct investigation of network structures, our understanding of them has been mainly from theoretical considerations. The first model calculation on randomly cross-linked networks was done by Tonelli and Helfand[9] for *cis*-1,4-polyisoprene (PIP). They calculated probability density functions to estimate the fraction of cross-links, as well as polymer, that are wasted in ends and loops. It was found that the weight fraction of elastically ineffective material is large and that the fraction of polymer contained in loops becomes significant for the case of solution curing. This result has provoked speculation that there might be some correlation between elastically ineffective material and the Mooney–Rivlin coefficient $2C_2$. More recently, Queslel and Mark[10] formulated a theory for the densities of active chains, active junctions, and the cycle rank for regular networks having only isolated ends. Their method is here extended to the case where chain scission is appreciable, which is especially the case for high-energy radiation.

Computer simulations prove to be powerful for network structure problems. Our previous work on end-linking systems shows that not only can the network structures[11,12] be well resolved by the use of simulation, but questions related to sol–gel transitions[13] and mechanical properties[11,14,15] can all be nicely addressed. Wherever there is sufficient knowledge of the reaction system and enough data for comparison, computer simulations can provide information with depth and accuracy that cannot be obtained in any other way.

We have modified our algorithms to enable us to simulate the simultaneous chain scission and cross-linking reactions that are induced by ionizing radiation. These studies have been performed for both bulk- and solution-cured PDMS systems, and the results will here be compared with experiments.[7,8] It will be demonstrated that computer model calculations can be used to great effect, even though there are very little available data to build upon.

2. Survey of Radiation Chemistry

Upon irradiation with high-energy radiation (electron beam or γ-ray), macromolecules will generally yield chain-end and side-chain macroradicals:

$$\sim\sim\sim\sim\sim\sim\sim\sim \xrightarrow{\text{irradiation}}$$

(1) main-chain scission $\quad \sim\sim\sim\sim\cdot + \cdot\sim\sim\sim\sim$

(2) side-chain dissociation $\quad \sim\sim\sim\sim\dot{\sim}\sim\sim\sim\sim + \cdot R_1$

Here $\cdot R_1$ is a fragment from the side chain of a macromolecule, which may be $\cdot CH_3$ or $\cdot H$ for PDMS. Solvent, if present, may also be dissociated. It should be noted that although we refer to these products as radicals, there is also evidence for ionic mechanisms from previous chemical studies.[2,4–6] Macroradicals can be deactivated by interaction with solvent molecules and fragment radicals, and new radicals can be generated by energy transfer and hydrogen abstraction. To form a cross-linkage, a side-chain macroradical recombines either with another to give a tetrafunctional cross-link or with a chain-end radical to yield a trifunctional junction. These two types of macroradicals are expected to have quite different reactivities, due to steric constraints and the cage effect. Cross-links with higher functionalities are also likely for some unsaturated polymers. This, however, is not believed to be the case[16] for PDMS.

The experimental data that are addressed by these simulations were reported[7,8] by Mark, Johnson, and Yu. PDMS with 6800 monomer units ($M_n = 0.5 \times 10^6$) was cross-linked with γ-radiation from a ^{60}Co source at room temperature. Various radiation doses were applied at

0024-9297/86/2219-2787$01.50/0

several different polymer concentrations to give a large set of samples. After irradiation, the networks were extracted, and their stress-strain isotherms were measured in both swollen and unswollen states. The measured sol fractions and mechanical property data are here to be compared with the model simulations.

3. Computer Model

In our calculations, all junctions are assumed to be tetrafunctional to facilitate comparisons with other theoretical calculations.[10,17] A number N_p of primary chains are randomly distributed in a cubical box, whose edge length L is determined from $L = (M_n N_p / \rho N_A V_p)^{1/3}$. Here, M_n is the number-average molecular weight of the primary chains, ρ is the density of the network, N_A is Avogadro's number, and V_p is the volume fraction of polymer in the system. We first generate the potential cross-linking and scission sites along the backbones of the primary chains, with chain lengths between these sites having a most probable distribution.[18] The distribution of distances between sites is Gaussian with one-dimensional variance given[14] by $\sigma^2 = C_n n l^2/3$, where n is the number of repeat units between sites, C_n is the characteristic ratio, and l is the length of one repeating unit. The parameter s, defined as the ratio of cross-linking sites to main-chain scission sites, measures the severity of chain scission.

Formation of cross-linkages in statistical configurations is controlled by varying a capture radius centered on each of the unreacted cross-linking sites in turn. Another radical that is within the capture sphere is allowed to form a cross-link with the one at the center, provided it is closer to the radical at the center than is any other. At the end of bond formation, the degree of cross-linking is recorded and chain scission occurs in proportion to the extent of cross-linking. The gel is then sorted from the sol by using a spanning tree[19] program, and its internal structure is probed. For a given configuration of molecules, the capture radius is increased step-by-step to span a range of extents of reaction, and molecular connectivities are recorded for each step.

Simulations were done for an ensemble of 800 primary chains, with the total number of active sites being about 29600. The size of this system is far greater than that used previously[11] for the end-linking systems (20000). No finite size effects were observed in those simulations. It is believed that results from this simulation should approach very closely to the limiting behavior for an infinite system. The computing time for a typical calculation with 20 capture radii is about 8 min on a Vax 11/780. Computations were performed at seven different polymer concentrations (100, 75, 62, 55, 48, 40, and 30%), and results averaging over four configurations for each are reported. Errors due to statistical fluctuations are less than 10% of the calculated quantities.

4. Results

The growth of the network upon irradiation is well explained by plotting gel fraction G as a function of the degree of cross-linking α, as shown in Figure 1, with $s = 5$. Here, G is the volume fraction of polymer incorporated into the gel, and α is the fraction of monomer units which are involved in the cross-linking reaction. In the figure, the results of simulations are illustrated by solid lines, with the percentages on the right indicating the initial polymer concentrations. In our study, gelation is first observed at $\alpha \simeq 0.05\%$, which is considerably larger than that of the Flory-Stockmayer theory[20] (0.015%) because of chain scission and loop formation. After that, polymer chains aggregate rapidly, and the gel fraction reaches a plateau

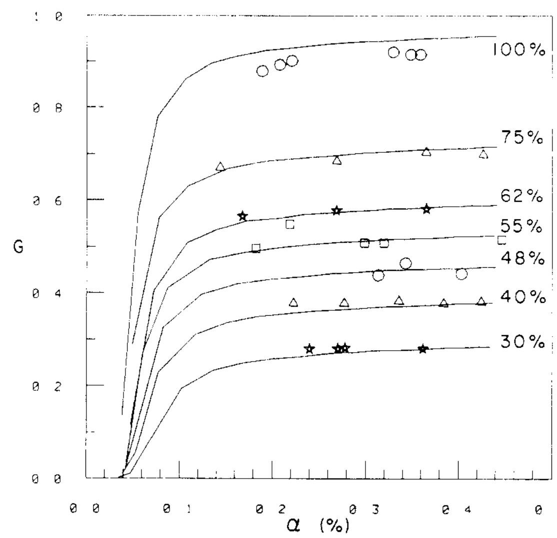

Figure 1. Gel fraction G vs. degree of cross-linking α for radiation-cured PDMS networks. Solid curves are from simulations, and symbols are estimated from experimental data.[7] Percentages on the right indicate the initial polymer concentrations.

at $\alpha \simeq 0.3\%$. The cross-linking and chain scission reactions have, apparently, reached steady state at this stage of reaction. In highly dilute solutions, gel formation is markedly reduced, a result implying increasing importance of intramolecular cross-linking.

The experimental results,[7] reported as G and $2C_1$, allow no direct comparison with simulations. A rough estimate of α can be made if M_c fulfills the relation[21]

$$M_c = \rho k T / (4C_1) \tag{1}$$

where M_c is the molecular weight between cross-links, k is Boltzmann's constant, and T is the temperature, and α is M_0/M_c, where M_0 is the molecular weight of the repeating unit. If experimental results are analyzed with the use of this relation, the values plotted as symbols in Figure 1 are obtained. These agree fairly well with our simulations. The agreement depends upon the value of s chosen. If we had allowed s to vary with concentration, better agreement could have been achieved. We were led to conclude that scission is very important for these networks because we could not force the simulations to agree with the data at all without some scission.

The cross-linking to scission ratio s used in this simulation is the same as q_0/p_0 defined by Charlesby,[1] where p_0 and q_0 are the probabilities that a randomly chosen monomer unit of the original polymer has undergone scission or is chemically cross-linked, respectively. The values of s reported in the literature are, unfortunately, rather diverse. Chain scission was first concluded[22] to be nonexistent or negligible with respect to cross-linking in the late 1950s. A model compound study[23] by St. Pierre, however, gave the ratio of 5. A similar result was also found[4] from in situ stress relaxation experiments by the same group. Later, Charlesby[2] replotted his and Miller's[16] solubility data to yield ratios of 12 and 8. Other studies by Langley[24] and by Kozlov[25] suggest values of 8 and 7.4, respectively. This ratio is found to be 3.5–4.5 when estimated from Mark's sol fraction data[7] according to Charlesby and Pinner's method.[1] One source of ambiguity was recognized[4] by Tanny and St. Pierre as radiation-induced SiO bond equilibrium. That is, there are actually more scissions than reported, but some scission products may exchange SiO bonds with other macromolecules, leaving the effect unobserved by most of the techniques that are used. The concentration and solvent dependence

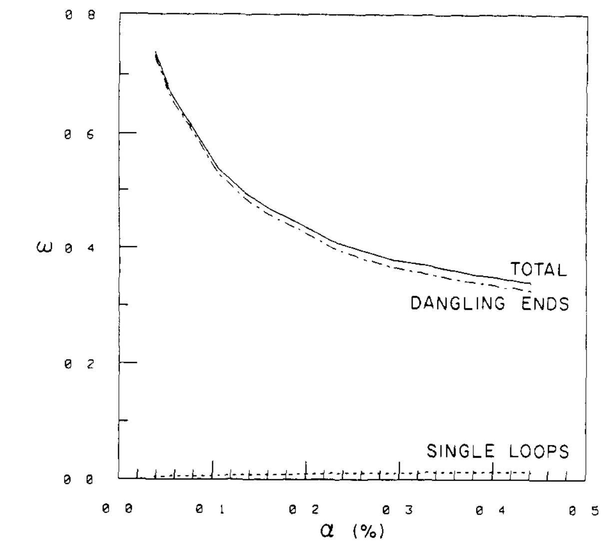

Figure 2. Weight fractions of dangling ends, single loops, and overall defect structures for a bulk-cured system.

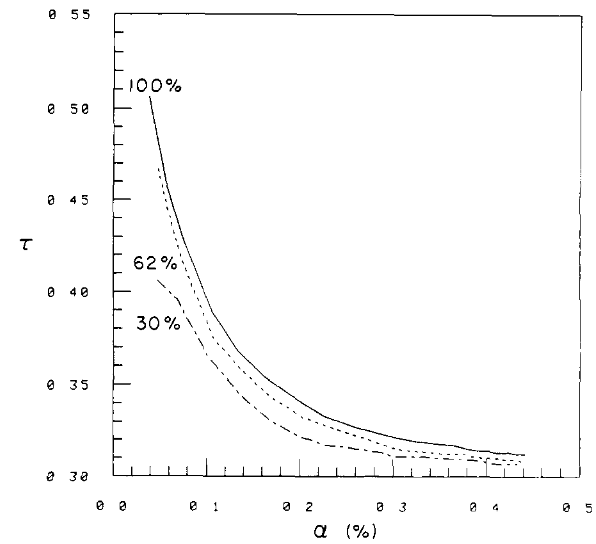

Figure 3. Number fractions of ends per chain, τ, vs. degree of cross-linking α for systems with 30, 62, and 100% polymer.

of this ratio has also been reported[3] for a variety of polymer systems. Schnabel investigated[26] the influence of concentration on the cross-linking and chain scissions for the PDMS + toluene system. It is unclear whether the cyclohexane that was used in the experiments[7,8] of Mark et al. would have a similar effect. With all these uncertainties, it is impossible to know exactly what this ratio should be. A tentative value of $s = 5$ is therefore used to show the general behavior. It is noted that this value is very close to that reported by St. Pierre and that deduced from the Mark et al. data, and it should be illustrative of what actually occurs in radiation cross-linking.

4.1. Dangling End Structures. Several structural irregularities are inherent in network topology; they can arise from initial ends, from chain scission, or from loop formation. Figure 2 shows the weight fractions ω of each of these individual components for a bulk system. The proportion of irregularities as a whole tends to decrease with increasing degree of cross-linking. This is reasonable since more chain segments are incorporated into the network as the extent of reaction increases. At $\alpha \simeq 0.4\%$, a typical degree of cross-linking for the networks prepared[7,8] by Mark et al., as much as 35% of the polymer segments are parts of defect structures, with 96% of these being chain ends. The remaining 4% are mainly single loops. For a more dilute system (30% polymer solution), the portion of defects is even higher, with 35.6% and 3.4% of the segments being wasted in ends and loops, respectively. The importance of dangling ends in this radiation-cured system is substantial. The calculations reported[9] by Tonelli and Helfand for the polyisoprene system yielded similar results. These observations strongly suggest that a careful consideration of the effects of defects is warranted, especially for networks that are randomly cross-linked by means of radiation.

The effect of dangling ends on network structure can be better understood through the number fraction of ends per chain, τ. These data are illustrated in Figure 3 for systems with 100%, 62%, and 30% concentration. In general, approximately half of the network chains are dangling ends when the network is just formed. This proportion decreases rapidly to a nearly constant value at $\alpha \simeq 0.3\%$, where about one-third of the chains are ends. The presence of this plateau is ascribable to the extent of chain scission. It is seen that one scission generates one subchain and two dangling ends. Each cross-linked unit, on the other hand, produces another subchain. In our simulation, cross-linking and chain scission take place simultaneously, with the ratio of cross-linked units to scissioned units being defined by s. If a total of N_r units react, there will be $2N_r/(s + 1)$ ends and N_r subchains created. Apart from the sol, the number of dangling ends would simply grow at a rate of $2/(s + 1)$ ends per chain. When the degree of cross-linking is high enough to smear out the effect of inherent ends, τ reaches an asymptotic limit, which is 0.333 for $s = 5$. It is noted that even at this asymptote, the network is still barely connected.

The slight dependence of τ on concentration has a peculiar origin. Upon chain scission, a loosely connected network made in dilute solution is likely to lose a relatively large portion of the network to the sol, which makes both the number of ends and subchains smaller in the gel. It appears that this subtle effect exerts an influence on the number of subchains in the network, which makes τ smaller for higher dilution.

The chain ends counted in Figure 3 are found in all sorts of environments. Either they may be isolated from one another (the "I" shape), or they may share cross-links with one or two other ends as in the letters "V" or "ψ". Their populations, represented by the number χ of structures per chain in the network, are displayed in Figure 4 for systems with 100% and 30% concentrations. As is clear from Figure 4, isolated ends are different from the other types in that their population increases, rather than decreases, with α. At the beginning of network formation, type V and ψ are favored, as follows from the elementary fact that most of the arms are due to initial ends. As network formation becomes more complete, the initial ends become isolated from one another, and the I type dominates. Chain scission dissects the incipient network at random, which again renders isolated ends highly probable. At $\alpha \simeq 0.4\%$, the populations of these ends reach an equilibrium, with a ratio of I:V:ψ of approximately 11:5:1. This ratio is relatively constant for more dilute systems. For the system with 30% polymer (Figure 4B), a ratio of 8:4:1 is obtained.

4.2. Loop Structures. The weight fraction of loops is small, as shown in Figure 2. Their number, represented by the fraction of cross-links κ involved in loop formation, is not negligible. Here, loops are defined as inactive closed paths that may implicate one (single loops), two (double-edge loops), or more strands. A plot of κ vs. α (Figure 5) for a 30% system reveals that as many as 50% of the cross-links are engaged in loops at low α. At higher ra-

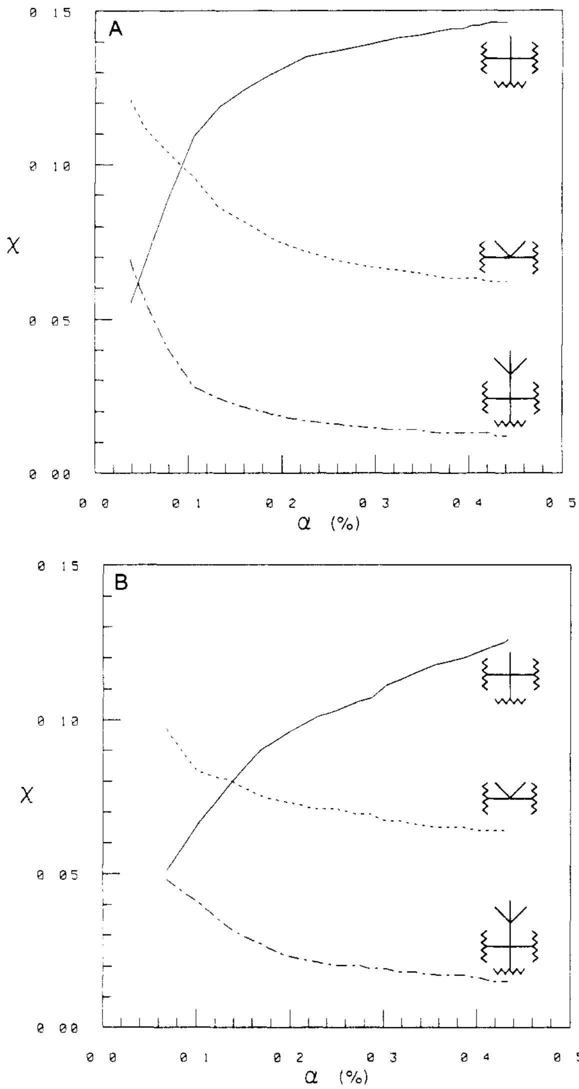

Figure 4. (A) Populations of end structures per chain, χ, for a bulk-cured system. Three different structures are reported here; they are referred to as types "I", "V", and "ψ", respectively, in the text. (B) Same as (A), but for a 30% polymer system.

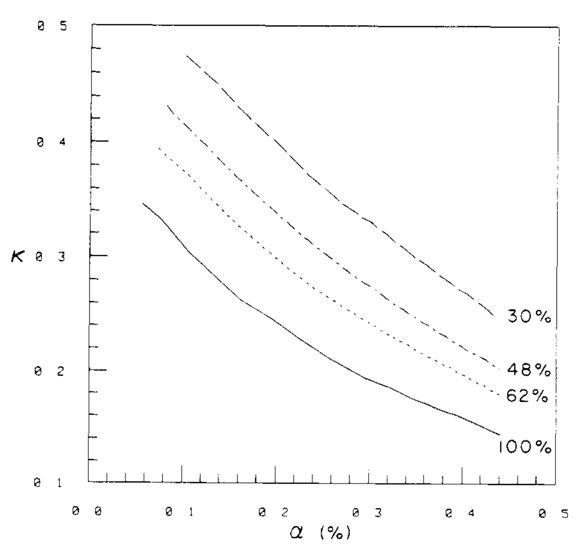

Figure 5. Fractions of cross-links κ that are involved in loop formation. Results are from simulations with 30, 48, 62, and 100% concentration.

diation doses, more effective circuits are formed, and this fraction is reduced substantially. In concentrated solu-

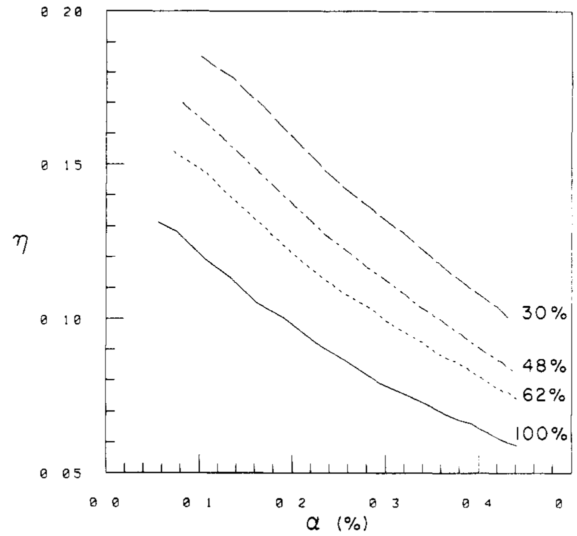

Figure 6. Populations of single loops per chain, η, plotted against α.

tions, loop formation becomes less probable. In the bulk, about 14% of the cross-links close loops at $\alpha = 0.44\%$, which is considerably smaller than in the 30% polymer system, where roughly 25% of the cross-links are found to be in the loops. This trend agrees well with that found[9] by Tonelli and Helfand. Our results for κ are also comparable with those for PIP, where 26% and 33% of these junctions have attached loops at $\alpha = 0.5\%$ for systems with 100% and 50% polymer.

Further analysis shows that more than 90% of the loops are single loops, the size of which increases with dilution. At $\alpha = 0.44\%$, the average single loop contains 38, 45, and 54 repeating units for systems having 100%, 48%, and 30% polymer. This is far less than the average number of monomers between cross-links (189). The fact that loops are relatively short reduces their weight percentage to marginal importance. It is interesting to note that the single loops that are formed in the polyisoprene calculations[9] are even shorter. At 100%, 50%, and 10% concentration, the average loop size (at $\alpha = 0.5\%$) is reported to be 24, 25, and 35, respectively. The higher loop formation found in those simulations probably resulted from the non-Gaussian statistics that were used for that work.

Loops can also be examined in the same manner as dangling ends. This is shown in Figure 6, where single loops per chain, η, are plotted against α. In the figure, the fraction of single loops is bounded within the range 0.13–0.18 at low degrees of cross-linking. At α approximately 0.44%, only 6–10% of the chains are in loops. It is noted that both single loops and ends per chain decrease with increasing cross-linking. They are different, however, in that no asymptote has been observed for η. On putting together Figures 2, 3, and 6, the whole picture of network formation becomes clear. For example, networks prepared in the bulk at $\alpha = 0.44\%$ have 31% of the chains in the ends and 6% in single loops, with their combined weight accounting for 34% of the network.

Other properties, such as the distribution of circuit lengths and viscoelastic relaxation spectra[14,15,27] among others, can be explored with the use of simulations. For the purpose of this work, these related topics are not pursued.

4.3. Mechanical Properties. The connection between the elastic free energy and cycle rank has been well developed by Flory.[28] For the simultaneous cross-linking and chain scission reactions simulated here, cycle ranks can be readily deduced. At any instant of irradiation, there are

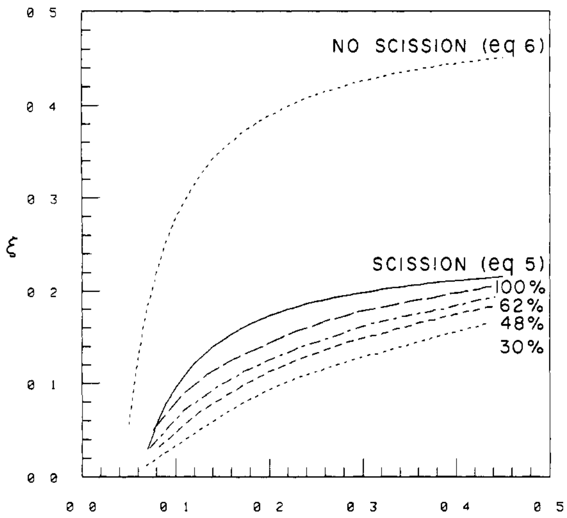

Figure 7. Cycle ranks per chain ξ obtained from simulations for systems with 30, 48, 62, and 100% polymer and from theoretical calculations with no loop formation (eq 5 and 6). The curve for eq 5 has a cross-linking/scission ratio of 5, but that of eq 6 assumes no chain scission.

ρ/M_n initial chains, ρ/M_c subchains, and $\rho/M_c - \rho/M_n$ reacted sites per unit volume. A fraction ν_c of these reacted sites is devoted to cross-linking

$$\nu_c = \frac{s\rho}{s+1}\left(\frac{1}{M_c} - \frac{1}{M_n}\right) \qquad (2)$$

and others are scissions

$$\nu_s = \frac{\rho}{s+1}\left(\frac{1}{M_c} - \frac{1}{M_n}\right) \qquad (3)$$

where s is the ratio of cross-linked sites to scissioned sites as before. If the cross-links are exclusively tetrafunctional, $\nu_c/2$ linkages are formed, with some of them being elastically inactive due to loop formation and nearby chain scissions. Each chain scission creates two more ends, in addition to the initial $2\rho/M_n$ ends. At a looping rate of η per chain, there will be $\eta\rho/M_c$ single loops per unit volume, where each loop produces an "equivalent" end. Assuming all chains are part of the network, the total number of non-end subchains μ is simply

$$\mu = \frac{\rho}{M_c} - 2\nu_s - 2\frac{\rho}{M_n} - \eta\frac{\rho}{M_c} \qquad (4)$$

The cycle rank per unit volume ξ_v is therefore $\xi_v = \mu - \nu_c/2$, according to Flory's theory.[17] Dividing ξ_v by ρ/M_c gives the cycle rank per chain ξ

$$\xi = \frac{1}{2(s+1)}\left\{(s-2) - \frac{3sM_c}{M_n}\right\} - \eta \qquad (5)$$

It is noted that this formulation takes care of the problem of inactive junctions automatically. Without chain scission ($s \rightarrow \infty$) and loop formation ($\eta = 0$) eq 5 reduces to Queslel and Mark's formula[10]

$$\xi = \tfrac{1}{2}\{1 - 3M_c/M_n\} \qquad (6)$$

Calculated values from eq 5 (with no loops and $s = 5$) and eq 6 are displayed in Figure 7. For systems with no scissions, the cycle rank per chain differs very little from that of the perfect network (0.5) at high extents of reaction. Once chain scission is included, dangling ends are produced in profusion, and the cycle rank decreases drastically. For example, at a degree of cross-linking of approximately 0.44%, the cycle rank is 0.215, which is less than half of that without scissions (0.450). In the real network, ξ is expected to be smaller, since loops do in fact form. This is exactly what is observed in Figure 7, where ξ is plotted against α for various systems. The cycle ranks for all these systems behave similarly, but their magnitudes depart all the more from eq 5 the more dilute is the concentration. This is obviously due to loop formation at high dilutions. The departures, however, are not uniform; they tend to be smaller at high degrees of cross-linking, which is consistent with the decreasing loop populations observed in Figure 6. The decrease in cycle rank is shown to be smaller than that suggested by eq 5 and Figure 6. This is attributed to the presence of sol, which makes an accurate formulation of ξ a very intricate problem.

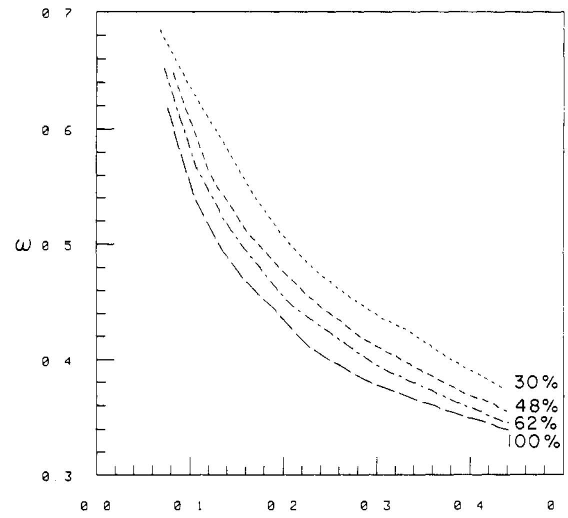

Figure 8. Weight fractions of elastically ineffective material in the network.

4.4. Ineffective Material and $2C_2$. Dangling ends and loops cannot support stress and are usually referred to as elastically ineffective material. A plot of their combined weight fraction ω vs. α, as illustrated in Figure 8, contains two important features. First, ω decreases with increased cross-linking, yielding 34–38% of the network as ineffective at $\alpha = 0.44\%$. This ratio is comparable to the PIP system,[9] where more than 50% of the network is found to be ineffective. Secondly, solution-cured systems tend to have more ineffective material than the bulk. The difference, mostly due to the highly populated loops in the solution and their large contours, is not large. At 30% concentrations, ω differs from that of the bulk by no more than 15%. This feature, which is also observed in the PIP system,[9] is pivotal to elucidating any possible correlation between ineffective material and the Mooney–Rivlin coefficient $2C_2$, as will be discussed below.

From experiments it is well-known that solution-cured networks have values at $2C_2$ which are much smaller than those of networks prepared from undiluted polymers. Swelling of networks by incorporation of a diluent, on the other hand, decreases $2C_2$ substantially. Just as a swelling agent dilutes the network, Tonelli and Helfand have conjectured[9] that the elastically ineffective portion of the polymer network might act as a diluent even in the absence of solvent. To verify this conjecture, comparisons of results derived from experiments[7,8] and from simulations are thought to be helpful. These comparisons are shown in Table I, where values of $2C_1$ and $2C_2$ in unswollen and swollen states are tabulated for each of two sets of samples. In the swollen state, dimethylsiloxane oligomer was used as the diluent at a volume fraction of 0.40. Samples in each

Table I
Representative Results from Experiments[7,8] and Simulations

concn, %	sample	unswollen state $2C_1$	unswollen state $2C_2$	swollen state[a] $2C_1$	swollen state[a] $2C_2$	α,[b] %	ξ[c]	ω[d]
				Set 1				
100	B-3	0.365	0.634	0.445	0.287	0.316	0.182	0.373
55	S3-2	0.361	0.445	0.387	0.240	0.326	0.162	0.392
40	S5-1	0.368	0.390	0.425	0.167	0.344	0.152	0.403
				Set 2				
75	S1-2	0.444	0.490	0.452	0.285	0.383	0.187	0.362
40	S5-2	0.458	0.400	0.485	0.235	0.415	0.170	0.378
30	S6-1	0.458	0.200	0.455	0.083	0.424	0.163	0.380

[a] Swollen in dimethylsiloxane oligomer to a volume fraction of diluent of 0.4. Values of $2C_1$ and $2C_2$ are in units of kg/cm^2. [b] Estimated from eq 1 and from the number of inactive cross-links observed in the simulation. [c] Cycle rank per chain. [d] Weight fraction of elastically ineffective material in the network.

set are selected to have the same (or similar) $2C_1$ for further comparisons. We have not included data which might be subjected to somewhat larger experimental errors.

We temporarily focus on the unswollen networks. If $2C_1$ is fixed, the cycle rank ξ should be almost constant. The same thing should be true for the fraction of ineffective chains, which is $1 - 2\xi$ according to Flory's theory.[17] Thus, if all these ineffective chains act as diluent, samples having the same $2C_1$ are expected to have similar $2C_2$. This, however, is not what is observed in experiments,[7,8] where values of $2C_2$ ranging from 0.634 to 0.390 are reported for sample set 1. Similar results are also found for set 2, where the variations are even larger. This evidence strongly suggests that a diluent effect cannot be the sole origin of $2C_2$. It is noteworthy that all these samples display a clear trend: $2C_2$ is smaller the more dilute is the solution at cure. The source of this trend might be traceable to the influence of solvent on subtleties of network topology that are presently beyond our ken.

From another point of view, if one assumes that variations of $2C_2$ in unswollen networks are mainly due to the diluent effect, the relation between diluent and ineffective network material should be quantifiable. As is clear from columns 4 and 6 of Table I, the value of $2C_2$ for sample B-3 is reduced from 0.634 to 0.287 upon swelling with 40% diluent. The latter quantity is smaller than that of a 40% solution-cured sample S5-1 in the unswollen state (0.390). The result implies that the difference between ineffective material for 40% solution-cured and bulk-cured networks is less than 40% diluent. The magnitude of this difference seems reasonable with respect to what is observed in Figure 8. There is, unfortunately, insufficient swelling data to render a more accurate estimate of this effect. Nevertheless, close inspection of $2C_2$ data from samples S5-2 and S6-1 reveals another story. The value of $2C_2$ measured in the unswollen state for a 30% solution-cured network S6-1 is found to be 0.200, which is even smaller than that of a 40% solution-cured network measured in the swollen state (0.235). The effect exerted by the difference of ineffective material between these two solution-cured samples (30% and 40%) is apparently more than that of 40% diluent. The magnitude of this difference is abnormally large when compared with that of Figure 8 and with the previous results from set 1. This inconsistency suggests that even if ineffective material were to act as a diluent, it cannot be solely responsible for the observed $2C_2$.

The simulation results for these samples are listed in the last three columns of Table I. The degree of cross-linking α is estimated from eq 1 and from the number of inactive cross-links that are formed; the cycle rank ξ and weight fraction of ineffective material ω are interpolated from Figures 7 and 8, respectively. Our values of ξ are roughly constant, which is expected since these samples are reported to have the same moduli. The scattering is small and may come from statistical fluctuations or from the fact that $2C_1$ is not really constant, as can be judged from the values in unswollen state (column 3) and swollen state (column 5). Despite this minor departure, it is gratifying that our simulations agree so closely with experiment. Further results to show that differences in ω are indeed quite small for all the samples are contained in the last column of Table I. For example, there is only a 0.2% difference between the weight fractions of ineffective material in samples S5-2 and S6-1. It is therefore hard to imagine how this tiny amount of ineffective material would work more effectively than 40% diluent to reduce the magnitude of $2C_2$.

5. Discussion

The simulations reported here clearly demonstrate that random networks cured by high-energy radiation have unique properties unlike those of other cross-linked systems. It is shown that defect structures account for a large portion of the networks and that their mechanical moduli, as represented by the cycle ranks per chain, are substantially smaller than those of end-linked networks.

Further evidence to show that chain scission is important can be derived from the experimental data reported by Mark et al.[7] It was observed that the gel fraction is practically constant beyond some critical dose, leaving a relatively constant sol content of about 7%. The high percentage of sol far exceeds that which can be ascribed to an impurity and strongly suggests the significance of scissions. It is noteworthy that the equilibrium between cross-linking and chain scissions is nicely preserved in our simulations, as can be seen from Figure 1. Simulations performed in the absence of chain scissions show that network formation occurs at α approximately 0.022%, which is slightly above that suggested by the classical theory. As the degree of cross-linking approaches 0.09%, sol fractions are found to be virtually zero. It was not possible for us to understand the experimental data without invoking chain scission.

St. Pierre attributes the wide range of reported s values to the presence of SiO bond equilibrium. If that is the case, the extents of SiO bond equilibria seem to differ quite a lot from one study to another. It is more likely that intricate mechanisms that are induced by the nonselective ionic radiation work collectively to give these highly diversified results. For instance, the cross-linking reaction is known to be governed by a diffusion-controlled mechanism. The primary chains used in those studies, however, have rather different molecular weights, which in turn have different diffusion coefficients. Main-chain scissions produce chain-end macroradicals. Some of these radicals can diffuse freely, while others are topologically connected to the network. Their reactivities are thought to be different. They may form cross-linkages, exchange SiO bonds, or simply deactivate to be dangling ends, depending on the local constraints. A comprehensive understanding of all these reaction rates and routes is thus a prerequisite for further fine tuning of the simulation model.

It should be noted that the good agreement of our results with experiments and with Tonelli's calculations manifests the credibility of these simulations. The interpretation of network structures in randomly cross-linked systems should be aided by results reported here, and the presumed correlation between elastically ineffective material and $2C_2$ should be settled as a consequence of this work.

Acknowledgment. This work was supported by the Department of Energy, Contract DE-FG06-84ER45123.

References and Notes

(1) Charlesby, A.; Pinner, S. H. *Proc. R. Soc. London, Ser. A* **1959**, *249*, 367.
(2) Ormerod, M. G.; Charlesby, A. *Polymer* **1963**, *4*, 459.
(3) Henglein, A.; Schnabel, W. *Curr. Top. Radiat. Res.* **1966**, *2*, 1.
(4) Tanny, G. B.; St. Pierre, L. E. *J. Phys. Chem.* **1971**, *75*, 2430.
(5) Lee, K. I.; Jopson, H. *Polym. Bull. (Berlin)* **1983**, *10*, 39.
(6) Kozlov, V. T.; Gur'ev, M. V.; Evseev, A. G.; Kashevskaya, N. G.; Zubov, P. I. *Vysokomol. Soedin., Ser. A* **1970**, *A12*, 592.
(7) Johnson, R. M.; Mark, J. E. *Macromolecules* **1972**, *5*, 41.
(8) Yu, C. U.; Mark, J. E. *Macromolecules* **1973**, *6*, 753.
(9) Tonelli, A. E.; Helfand, E. *Macromolecules* **1974**, *7*, 59, 832.
(10) Queslel, J. P.; Mark, J. E. *J. Chem. Phys.* **1985**, *82*, 3449.
(11) Leung, Y. K.; Eichinger, B. E. *J. Chem. Phys.* **1984**, *80*, 3877, 3885.
(12) Shy, L. Y.; Eichinger, B. E. *Br. Polym. J.* **1985**, *17*, 200.
(13) Shy, L. Y.; Leung, Y. K.; Eichinger, B. E. *Macromolecules* **1985**, *18*, 983.
(14) Eichinger, B. E. *J. Chem. Phys.* **1981**, *75*, 1964.
(15) Neuberger, N. A.; Eichinger, B. E. *J. Chem. Phys.* **1985**, *83*, 884.
(16) Miller, A. A. *J. Am. Chem. Soc.* **1960**, *82*, 3519.
(17) Flory, P. J. *Macromolecules* **1982**, *15*, 99.
(18) Tanny, G. B.; St. Pierre, L. E. *J. Polym. Sci., Part B* **1971**, *9*, 863.
(19) Nijenhuis, A.; Wilf, H. S. *Combinatorial Algorithms*; Academic Press: New York, 1975; Chapter 18.
(20) Flory, P. J. *Principles of Polymer Chemistry*; Cornell University: Ithaca, NY, 1953; p 358.
(21) Chiu, D. S.; Mark, J. E. *Colloid Polym. Sci.* **1977**, *254*, 644.
(22) Chapiro, A. *Radiation Chemistry of Polymeric Systems*; Interscience: New York, 1962; Chapter 9.
(23) Dewhurst, H. A.; St. Pierre, L. E. *J. Phys. Chem.* **1960**, *64*, 1063.
(24) Langley, N. R.; Polmanteer, K. E. *Polym. Prepr. (Am. Chem. Soc., Div. Polym. Chem.)* **1972**, *13*, 235.
(25) Kozlov, V. T.; Evseev, A. G.; Zubov, P. I. *Vysokomol. Soedin., Ser. A.* **1969**, *A11*, 2230.
(26) Schnabel, V. W. *Makromol. Chem.* **1967**, *103*, 103.
(27) Martin, J. E.; Eichinger, B. E. *Macromolecules* **1980**, *13*, 626.
(28) Flory, P. J. *Proc. R. Soc. London, Ser. A* **1976**, *351*, 351.

Studies of the Antenna Effect in Polymer Molecules. 10. Preparation and Luminescence Studies of Sulfonated Poly(2-vinylnaphthalene)

James E. Guillet,* Jiayuan Wang,† and Liying Gu‡

Department of Chemistry, University of Toronto, Toronto, Canada M5S 1A1.
Received January 13, 1986

ABSTRACT: Partial sulfonation of poly(2-vinylnaphthalene) (P2VN) yields water-soluble copolymers (SP2VN) that appear to exhibit hypercoiling in aqueous media. Luminescence emission studies show that excimer emission is much higher in aqueous solution than in conventional organic solvents, presumably because of closer packing of the naphthalene groups in the interior of the hydrophobic "core". Photon-counting measurements of fluorescence decay are consistent with very rapid migration and trapping of singlet energy in the hypercoiled conformation. Evidence is also presented for the preferential trapping of large aromatic groups such as perylene in the interior of the coil. Luminescence emission depends strongly on the pH and ionic strength of the medium. In frozen aqueous media at 77 K delayed emission is almost exclusively from the naphthalene excimer rather than from the "monomer" as in conventional solvents, thus confirming the ease of population of excimer sites in hypercoiled conformations.

In previous studies in this series it has been shown that polyelectrolytes containing large aromatic chromophores such as naphthalene behave as if they are "hypercoiled" in dilute aqueous solution, such that the hydrophobic aromatic groups are clustered near the center of the polymer coil, while the hydrophilic ionic groups are located on the exterior.[1,2] The first report of this work was given by Guillet and co-workers in 1981.[1] In these early studies, the polymers used were copolymers of acrylic acid containing minor quantities (8–22 mol %) of naphthylmethyl methacrylate (NMMA) which were end-trapped with anthracene to demonstrate the efficiency of energy transfer. The much higher efficiency of singlet energy migration and trapping that occurred when these polymers were dissolved in aqueous media (as compared to organic solvents) was explained as being the result of hypercoiling to form a pseudomicellar conformation in which the hydrophobic aromatic groups form the core, stabilized by hydrogen bonding, and the inorganic carboxyl groups are located on the exterior.

These conclusions have been confirmed by more recent work of Itoh et al.[3] and Morishima et al.,[4] who studied the quenching of fluorescence from amphiphilic copolymers of 2-acrylamido-2-methylpropanesulfonic acid (AMPS) with vinyl aromatic monomers. On the basis of the increased emission of the amphiphilic probe 8-anilino-1-naphthalenesulfonate (ANS) and the higher quenching efficiency of the hydrophobic quencher bis(2-hydroxyethyl) terephthalate (BHET), it was concluded that the polymer

† Current address: South China Institute of Technology, Guangzhow, People's Republic of China.
‡ Current address: Institute of Chemistry, Academia Sinica, Beijing 100 080, People's Republic of China.

